Alloying of C40-structured Mo(Si,Al)<inf>2</inf> with Nb, Ta and V

Materials Letters 353 (2023) 135219

Contents lists available at ScienceDirect

Materials Letters

journal homepage: www.elsevier.com/locate/matlet

Alloying of C40-structured $Mo(Si,Al)_2$ with Nb, Ta and V

Aina Edgren [a,b], Erik Ström [a], Anand Rajagopal [c], Magnus Hörnqvist Colliander [a,*]

[a] Department of Physics, Chalmers University of Technology, Gothenburg SE-41296, Sweden
[b] Kanthal AB, SE-73427 Hallstahammar, Sweden
[c] Alleima AB, SE-81181 Sandviken, Sweden

ARTICLE INFO

Keywords:
$Mo(Si,Al)_2$
Alloying
X-ray diffraction
Electron-probe microanalysis
Energy-dispersive X-ray spectroscopy

ABSTRACT

Alloying of $Mo(Si,Al)_2$, prepared by sintering, with Nb, Ta or V has been studied. All alloyed materials retained the C40-structured matrix phase of the un-alloyed reference material. The concentration of alloying elements in the C40 phase reached 0.4–1.6 at.% (approximately 20–50 % of the intended levels), and the remaining alloying content was dissolved in the minority $D8_m$- and $D8_8$-structured $(Mo,X)_5(Si,Al)_3$ phases. V-alloying also promoted the formation of C54-structured $(Mo,V)(Si,Al)_2$.

1. Introduction

$Mo(Si,Al)_2$ is a ceramic material with excellent oxidation properties [1,2] used for resistive heating elements in demanding environments, and thus presents an attractive candidate for electrification of fossil-fuel-based industrial heating processes. However, the necessary upscaling to MW operation and geometrical constraints in such applications require improved high-temperature mechanical properties. While the strength of $Mo(Si,Al)_2$ decreases continuously with increasing temperature, other disilicides with the same crystal structure (Strukturbericht designation: C40), $NbSi_2$, $TaSi_2$ and VSi_2, show an anomalous increase in strength at high temperatures [3–5]. This raises the question if a similar effect could be achieved by alloying $Mo(Si,Al)_2$ with these elements. However, transition metal alloying of $Mo(Si,Al)_2$ has not received much attention so far, and the first question is whether it is possible to incorporate the alloying elements into the C40 phase. In this study, we investigate the potential for alloying of $Mo(Si,Al)_2$ with the proposed strengthening elements Nb, Ta and V.

2. Materials and characterisation

One reference and four alloyed materials ($(Mo_{0.95}Nb_{0.05})(Si,Al)_2$, $(Mo_{0.9}Ta_{0.1})(Si,Al)_2$, $(Mo_{0.95}V_{0.05})(Si,Al)_2$, and $(Mo_{0.9}V_{0.1})(Si,Al)_2$, referred to as 5Nb, 10Ta, 5V and 10V, respectively) were prepared by dry mixing of elemental powders. The mixed powders were heated in Ar gas to initiate an exothermic, self-propagating reaction in which $Mo(Si,Al)_2$ is formed. The reaction also leads to the formation of small amounts of $Mo_5(Si,Al)_3$ due to local chemical variations in the unreacted powder [6]. The reaction products were milled, and 3 wt% Al_2O_3 powder was added to the alloyed powders to inhibit grain growth during sintering. The addition will not affect the microstructure in other ways, due to the high stability of the oxide [7]. The powders were compacted using cold isostatic pressing, before sintering for 1 h at 1600–1610 °C in H_2 gas. The density of the sintered materials was 5.75 (reference), 5.71 (5Nb), 5.90 (10Ta), 5.59 (5V) and 5.41 g/cm^3 (10V).

Cross-sections of the materials were cut, ground and polished using SiC paper, diamond solutions and colloidal silica prior to microstructure characterisation using scanning electron microscopy (SEM) based methods: backscattered electron (BSE) and secondary electron (SE) for imaging; energy-dispersive X-ray spectroscopy (EDS) (20 kV) and electron-probe microanalysis with wavelength-dispersive X-ray spectroscopy (EPMA/WDS) (10 kV) for chemical composition; and electron backscatter diffraction (EBSD) (15 kV) for phase identification. Synchrotron X-ray diffraction (SXRD) was performed at the P02.1 (10V material, wavelength 0.207 Å) and the P21.2 (all other materials, wavelength 0.151 Å) beamlines at PETRA III, DESY. The diffracted signal was collected in transmission using downstream area detectors calibrated by standards. Rietveld refinements were performed on the reduced data in GSAS-II [8].

3. Results and discussion

The majority phase in all materials is C40, and α-Al_2O_3, $D8_m$- and $D8_8$-structured $(Mo,X)_5(Si,Al)_3$ are present as minority phases (Fig. 1).

* Corresponding author.
E-mail address: magnus.colliander@chalmers.se (M. Hörnqvist Colliander).

https://doi.org/10.1016/j.matlet.2023.135219
Received 16 June 2023; Received in revised form 25 August 2023; Accepted 11 September 2023
Available online 16 September 2023

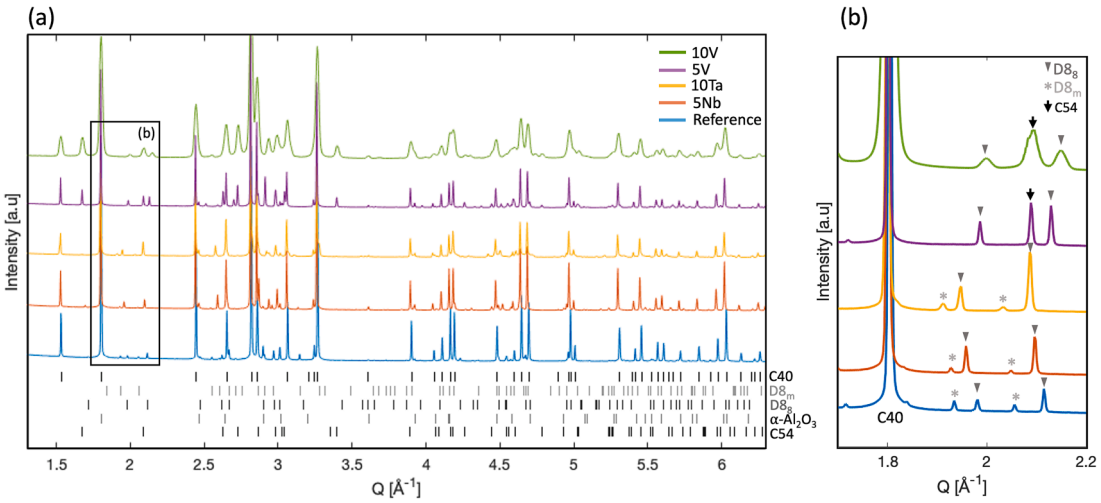

Fig. 1. (a) SXRD of all materials, (b) close-up showing C40, $D8_m$, $D8_8$ and C54 peaks. Note that the larger peak width in 10V is a result of lower instrumental resolution and not sample-related broadening.

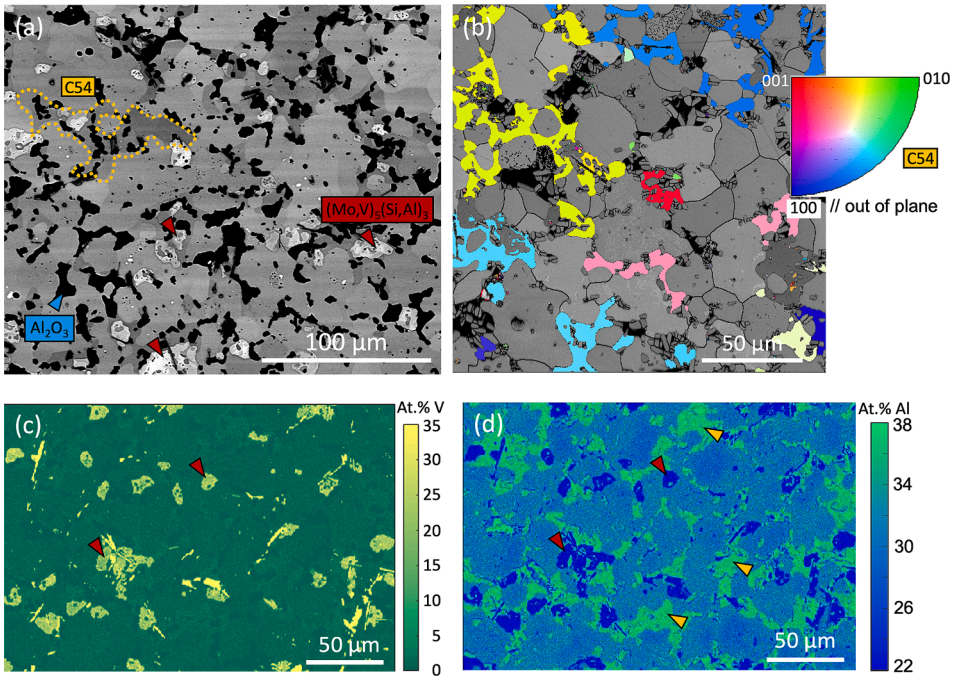

Fig. 2. Microstructure of the 10V sample. (a) BSE image, (b) EBSD IPF map of the C54 phase, where the colour indicates the crystallographic axis aligned with the out-of-plane direction. (c) EPMA V map, and (d) EPMA Al map. The matrix phase is C40. Yellow, red, and blue arrows indicate C54, $Mo_5(Si,Al)_3$ and Al_2O_3 grains, respectively (identified by combinations of BSE contrast, EDS, and EBSD).

$D8_m$ is often reported as a secondary phase in $Mo(Si,Al)_2$ materials [2,6], and $D8_8$ is stabilised by carbon [9,10]. In addition, a C54-structured Mo $(Si,Al)_2$ phase is present in the V-alloyed materials. This will be discussed later.

All materials consist of a C40 matrix phase with Al_2O_3 and (Mo, $X)_5(Si,Al)_3$ particles distributed throughout. This is exemplified by the BSE image of 10V in Fig. 2(a). BSE images and EDS maps of all materials are found in the supplementary material (Figures S1-S5). The phase volume fractions obtained from a combination of Rietveld refinements (see Figures S6-S10 in the supplementary material) of the SXRD data and image analysis of BSE and SE images show that the materials contain roughly 75–85 vol% C40. The remaining fraction consists of Al_2O_3 (around 10–15 vol%) and minor amounts of $D8_8$ and $D8_m$. The C40 fraction is slightly lower in the V-alloyed materials, around 70 vol%, where C54 accounts for around 10–15 vol%. The C54 grains have an elongated structure (Fig. 2(b)) and will be discussed later in this letter.

Table 1
Chemical composition of C40 acquired using EPMA (at.%) (uncertainty).

Material	Mo	X	Si	Al
Reference	31.6(5)		36.6(5)	31.8(3)
5Nb	34.7(4)	0.55(4)	33.9(2)	30.9(3)
5V	36.7(9)	0.39(6)	29.3(5)	33.4(6)
10V	29.8(3)	0.9(2)	37(1)	32(1)
10Ta	34.2(7)	1.6(2)	35.4(5)	28.9(4)

The chemical composition of C40 (Table 1) shows that the concentration of alloying elements in C40 is low, between 0.39 and 1.55 at.%.

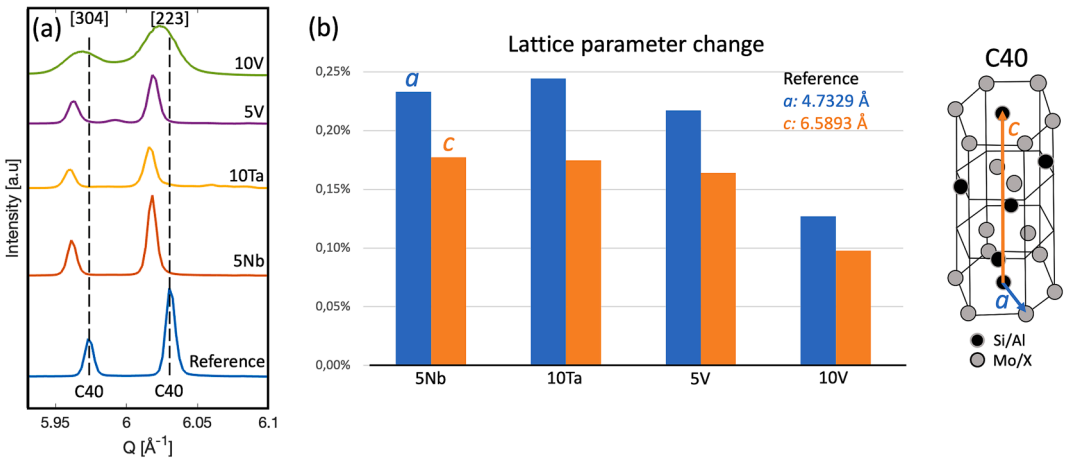

Fig. 3. (a) SXRD diffractogram of two C40 peaks. (b) Comparison between lattice parameters of alloyed materials and the reference.

Small amounts of C and O were detected (up to 3.24 and 1.37 at.% C and O, respectively). These were not added on purpose, but are probably contaminations from the synthesis, which cannot be avoided in powder processing of ceramics. The O content is probably due to the presence of nano-sized Al_2O_3 particles distributed within the C40 grains, which have previously been found in the reference material [11]. The chemical compositions in Table 1 were calculated without considering C, and with the Al concentration corrected to account for the presence of Al_2O_3 (i.e., Al was reduced by 2/3 of the O concentration). The chemical composition including C and O is found in the supplementary materials (Table S1).

The maximum attainable concentration of the alloying elements in the C40 phase (assuming a full solubility in single-phase C40 material) is 1.7 at.% in the case of 5X materials and 3.3 at.% for 10X materials. Table 1 shows that the concentration reaches approximately 20–50 % of these (intended) levels (33 % in 5Nb, 47 % in 10Ta, 23 % in 5V and 25 % in 10V). In the V-alloyed materials, the C54 phase contains similar amounts of V (0.34 at.% in 5V and 1.7 at.% in 10V) as the C40 phase. The remaining alloying content is dissolved in the minority phases $D8_m$ and $D8_8$, which contain up to 38 at.% alloying elements, as exemplified by the EPMA map in Fig. 2(c) and seen in the EDS maps in Figures S1-S5 in the supplementary material. Based on these results, the alloying potential of C40 can be argued to be limited, unless the formation of $(Mo,X)_5(Si,Al)_3$ can be avoided during processing. On the other hand, the V content in C40 is higher (approximately twice as high) in 10V compared to 5V, suggesting that the maximum solubility has not been reached.

All materials have slightly (up to 0.25 %) larger lattice parameters than the reference material ($a = 4.73292(6)$ Å, $c = 6.58929(7)$ Å), see Fig. 3. As Nb, Ta and V occupy the same sites in C40 XSi_2 as Mo does in $Mo(Si,Al)_2$, the alloying elements are expected to substitute for Mo in $(Mo,X)(Si,Al)_2$. Considering the relative atomic radius of the alloying elements with respect to Mo, Nb and Ta alloying should result in larger lattice parameters, whereas V should lead to a decrease. Therefore, it is not likely that the changes in the lattice parameter are only caused by the direct effect of the alloying elements on the lattice, but also by variations in stoichiometry (Table 1). Whether these variations are induced by the alloying or by the processing cannot be determined without dedicated studies.

The C54-structured $(Mo,V)(Si,Al)_2$ present in the V-alloyed materials has previously been observed in Al-rich $Mo(Si_{1-x}Al_x)_2$ materials, $x > 0.5$ [6,12], and has been suggested to form via a peritectic reaction between liquid, C40 and Mo_5Si_3 [13,14]. The morphology of the C54 grains in 5V and 10V (see Fig. 2(b), where individual C54 grains extend as networks surrounding C40 grains) suggests that it crystallized from a melt during the cooling after sintering, which agrees with the proposed peritectic reaction. Since C54 is only present in the V-alloyed materials, with a higher fraction in 10V compared to 5V, V seems to promote its formation. As C54 forms from the liquid phase, this could be related to a possible reduction in the melting temperature by V additions, considering that for pure disilicides the melting point of VSi_2 (1677 °C) is considerably lower than that of $NbSi_2$ (1940 °C), $TaSi_2$ (2040 °C) and $MoSi_2$ (2030 °C) [3,15]. The melting point of $Mo(Si,Al)_2$, and how it is affected by alloying, is still not known. The Al-content in C54 is higher than in C40 (Fig. 2(d)), in agreement with previous reports [6,12].

4. Summary

We have investigated the possibility of alloying C40-structured $Mo(Si,Al)_2$ with Nb, Ta and V. In summary, the following observations have been made:

- $(Mo,X)(Si,Al)_2$ retains the C40-structure when alloyed.
- The alloying element concentration in the C40 phase reached some 20–50 % of intended levels, with the remaining alloying content being dissolved in the minority phases $D8_m$ and $D8_8$.
- V-alloying promotes the formation of C54-structured $(Mo,V)(Si,Al)_2$.

CRediT authorship contribution statement

Aina Edgren: Conceptualization, Methodology, Investigation, Writing – original draft, Visualization. **Erik Ström:** Conceptualization, Resources, Writing – review & editing, Supervision. **Anand Rajagopal:** Investigation, Resources. **Magnus Hörnqvist Colliander:** Conceptualization, Writing – review & editing, Supervision, Project administration, Funding acquisition.

Declaration of Competing Interest

The authors declare that they have no known competing financial interests or personal relationships that could have appeared to influence the work reported in this paper.

Data availability

Data will be made available on request.

Acknowledgements

This research was funded by the Swedish Foundation for Strategic Research (SSF) and Kanthal AB, through the industrial PhD student grant ID18-0064. The work was performed in part at Chalmers Analysis Laboratory (CMAL). We acknowledge DESY (Hamburg, Germany), a

member of the Helmholtz Association HGF, for the provision of experimental facilities. Parts of this research were carried out at PETRA III and we would like to thank Dr. Ulrich Lienert for assistance in using beamlines P21.1, and Dr. Martin Etter for performing the rapid access measurements at P02.1 Beamtime was allocated for proposal I-20211111 EC and RAt-20010296.

Appendix A. Supplementary data

Supplementary data to this article can be found online at https://doi.org/10.1016/j.matlet.2023.135219.

References

[1] L. Ingemarsson, K. Hellström, S. Canovic, T. Jonsson, M. Halvarsson, L. G. Johansson, J.E. Svensson, J. Mater. Sci. 48 (2013) 1511–1523.
[2] L. Ingemarsson, K. Hellström, L.G. Johansson, J.E. Svensson, M. Halvarsson, Intermetallics 19 (2011) 1319–1329.
[3] Y. Umakoshi, T. Nakano, K. Kishimoto, D. Furuta, K. Hagihara, M. Azuma, Mater. Sci. Eng. A 261 (1999) 113–121.
[4] H. Inui, M. Moriwaki, M. Yamaguchi, Intermetallics 6 (1998) 723–728.
[5] M. Moriwaki, K. Ito, H. Inui, M. Yamaguchi, Mater. Sci. Eng. A 239–240 (1997) 69–74.
[6] M. Esmaeili Ghayoumabadi, A. Saidi, M.H. Abbasi, J. Alloy. Compd. 472 (2009) 84–90.
[7] A. Edgren, E. Ström, L. Frisk, F. Akhtar, M. Hörnqvist Colliander, Mater. Sci. Eng. A (2023) 865.
[8] B.H. Toby, R.B. Von Dreele, J. Appl. Cryst. 46 (2013) 544–549.
[9] G. Zhang, X. Yue, J. Mater. Sci. 35 (2000) 4729–4733.
[10] E. Parthe, W. Rieger, J. Dent. Res. 47 (1968) 829–835.
[11] A. Edgren, E. Ström, R. Qiu, L. Frisk, F. Akhtar, M. Hörnqvist Colliander, Mater. Sci. Eng. A 849 (2022), 143387.
[12] T. Tabaru, K. Shobu, M. Sakamoto, S. Hanada, Intermetallics 12 (2004) 33–41.
[13] N. Ponweiser, W. Paschinger, A. Ritscher, J.C. Schuster, K.W. Richter, Intermetallics 19 (2011) 409–418.
[14] Y. Liu, G. Shao, P. Tsakiropoulos, Intermetallics (2000).
[15] K. Ito, H. Inui, Y. Shirai, M. Yamaguchi, Philos. Mag. A Phys. Condens. Matter, Struct. Defects Mech. Prop. 72 (1995) 1075–1097.